ELSEVIER

Physica A 224 (1996) 188–198

PHYSICA A

Criticality in driven cellular automata with defects

Bosiljka Tadić [a], Ramakrishna Ramaswamy [b]

[a] *Jožef Stefan Institute, P.O. Box 100, 61111 Ljubljana, Slovenia*

[b] *School of Physical Sciences, Jawaharlal Nehru University, New Delhi 110067, India*

Abstract

We study three models of driven sandpile-type automata in the presence of quenched random defects. When the dynamics is conservative, all these models, termed the random sites (A), random bonds (B), and random slopes (C), self-organize into a critical state. For model C the concentration-dependent exponents are nonuniversal. In the case of nonconservative defects, the asymptotic state is subcritical. Possible defect-mediated nonequilibrium phase transitions are also discussed.

1. Introduction

Self-organized criticality (SOC) [1] is a dynamic phenomenon which occurs in certain dissipative systems with large numbers of degrees of freedom. Such a system, when slowly driven into its metastable state, self-organizes in a state with long-range correlations, similar to the critical state at a second-order phase transition.

In conventional criticality, quenched disorder can be a *relevant* perturbation in the vicinity of the critical point. It is therefore natural to ask how the SOC state responds to similar perturbations. One might expect that self-organizing systems are more robust against random perturbations, since the critical state is an attractor of the dynamics, although the universality class may change in presence of disorder.

We explore this question in the present work, where we demonstrate, using numerical simulations on simple models of self-organizing cellular automata with frozen random defects, the conditions for a system to self-organize, and determine the universality class of the critical behavior. Disorder-mediated phase transitions between different types of metastable states are also discussed.

We study three kinds of random defects which locally affect the rules of relaxation in a manner analogous to the random site, random bond, and random field defects in spin models displaying conventional critical phenomena. All these models are based on the

0378-4371/96/$15.00
SSDI 0378-4371(95)00322-3

Table 1
Critical exponents and mass-to-scale ratio in 2D directed models with defects

Model	$D_{\|\|}$	θ	τ	α	z	ϕ	μ	τ_n	D_n	Remark
A	3/2	1/2	1/3	1/2	1	1/2	1	1/3	3/2	universal
B	1.62	1.04	0.65	1.04	1	none	1.006	0.466	1.997	universal
C	1.49	0.57	0.38	0.54	1.002	none	0.978	0.366	1.54	nonuniversal

directed abelian 2-dimensional *critical height* model (toppling if $h(i,j) \geq h_c$) which is exactly solvable in the absence of defects [2], in which the dynamic rules are locally modified at a fraction c of "defect" sites. In model A, holes of infinite depth are placed at random sites. In model B there are two variables $h_1(i,j)$ and $h_2(i,j)$ associated with each site (i,j). These are coupled at random sites (details are given in Section 3 below), in a manner so as to lead to a multiplicity of metastable states, as in the case of spin-glasses and other frustrated systems. In model C, frozen-in local slopes are introduced by preventing relaxation through the height instability at defect sites, and instead applying a critical slope toppling rule at all sites with slopes $\sigma(i,j) \geq \sigma_c$. In this case, regions with local slopes $\sigma(i,j) \sim \sigma_c$ are established, while the rest of the system relaxes according to the critical height rule (the critical height h_c is chosen such that $h_c < \sigma_c$). In all three cases the ratio between the number of particles leaving one site and the number appearing at its neighbors is not uniform at defect sites.

The numerical results presented here are from simulations on lattices (with periodic boundary conditions in the transverse direction) of size $12 \leq L \leq 384$ for time steps (see below) up to 1×10^6. A lattice with frozen-in defects is prepared and kept fixed for the entire number of time steps, and then a new configuration is prepared; results are then averaged over the total number of configurations. In each case, the system was driven by randomly adding particles to sites at the top (first row), $h(1,j) \to h(1,j)+1$.

2. Subcriticality: random-site model (A)

The dynamic height variable $h(i,j)$, associated with each lattice site (i,j) on a square lattice, is updated according to the rules of the critical height model: if $h(i,j)$ exceeds a critical value h_c, then the site is unstable and relaxes according to

$$h(i,j) \to h(i,j) - 2, \qquad h(i+1,j_\pm) \to h(i+1,j_\pm) + 1, \tag{1}$$

where $(i+1,j_\pm)$ are the two neighboring downstream sites. This rule applies to all sites except for a fraction c of randomly distributed defect sites, at which infinitely deep holes are placed. Thus two grains are lost each time an avalanche hits a defect, rendering the dynamic process nonconservative. (Similar nonconservative models have been considered earlier [3]). For $c = 0$ the critical exponents are listed in Table 1. An annealed version of defects of the above type was studied numerically in Ref. [4], where it was shown that the system self-organizes into a subcritical state. The probability

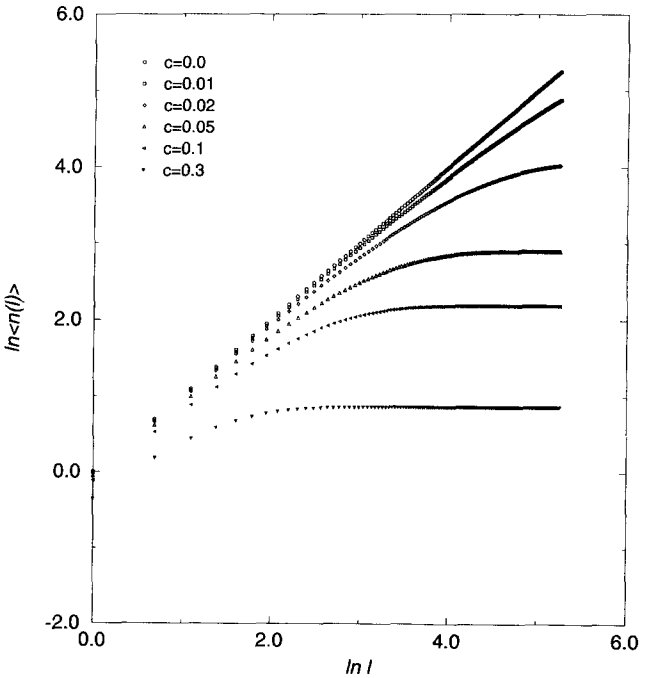

Fig. 1. Time average of the number of topplings $\langle n(l)\rangle$ vs. distance l from the top of pile for various concentrations of defects c.

distributions of duration $P(t,c)$ and size $D(s,c)$ were found to fulfill the following scaling forms:

$$P(t,c) = t^{-\alpha}\mathcal{P}(t/\xi_t(c)), \qquad D(s,c) = s^{-\tau}\mathcal{D}(s/\xi_s(c)), \tag{2}$$

where the correlation lengths $\xi_t(c) \sim c^{-\mu_t}$ and $\xi_s(c) \sim c^{-\mu_s}$ for time and spatial correlations, respectively, diverge in the limit $c \to 0$, with $\mu_t = 1$ and $\mu_s = 1.5$ [4,5]. The scaling functions defined in Eq. (2) were calculated numerically in Ref. [4]. With the dynamical rules (1) there are no recurrences in the avalanche dynamics and thus both annealed and quenched (frozen) impurities lead to the same universal scaling properties. In Fig. 1 we plot $\langle n(l)\rangle$, the average number of particles relaxed[1] up to distance l (measured from the top of the pile) for various values of the defect concentration:

In the absence of defects $\langle n(l)\rangle$ is proportional to the average number of toppled sites $\langle s(l)\rangle$ and thus exhibits a power-law behavior

$$\langle n(l)\rangle \sim l^{\mu}, \tag{3}$$

[1] The number of particles relaxed up to distance l is the total number of particles that take part in the relaxation processes from the top of pile up to the lth row. For lattices with defects, this quantity need not be the same as the total number of toppled sites.

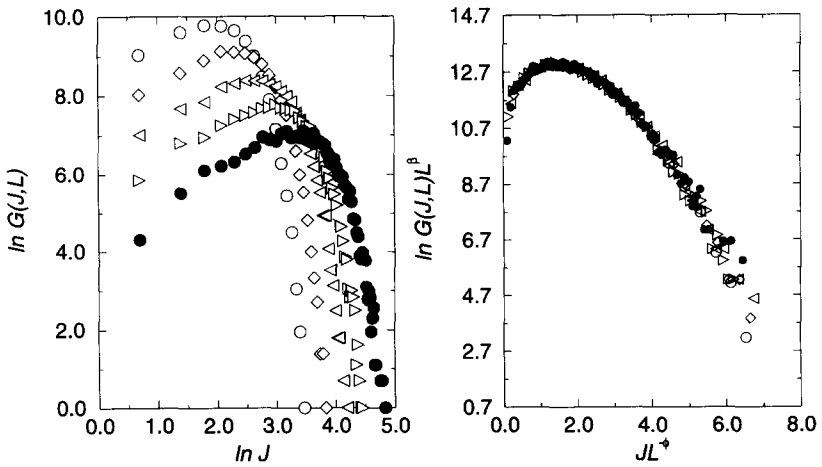

Fig. 2. Outflow current distribution in the absence of defects for system sizes $L = 24$, 48, 96, 192, and 384 (left), and the corresponding finite-size scaling plot (right).

with $\mu = 1$ (cf. the top curve in Fig. 1). For finite concentration of defects c, the curve flattens, and the scaling region with slope μ decreases with increasing c, corresponding to the decreasing correlation length in the system. At a critical concentration $c = c^* = 0.295 \equiv 1 - p_d$, the directed-percolation threshold [6], it is no longer possible to have a lattice spanning cluster [4].

For sandpiles without defects, the fluxes into and out of the lattice are equal – the distribution $G(J, L)$ of the current which flows over the rim of the system is shown in Fig. 2 for $c = 0.0$ and various systems sizes L. As expected for a self-organized critical state, the outflow current distribution exhibits scale invariance [7], i.e.

$$G(J, L) = L^{-\beta} \mathcal{G}(J/L^{\phi}). \tag{4}$$

The finite-size scaling fit, also shown in Fig. 2, has the exponents $\beta = 1$ and $\phi = 0.5$. With defects, the outflow current diminishes with increasing concentration of defects, eventually vanishing at $c = c^*$ (see Section 5). There is no apparent scaling form of $G(J, c)$.

3. Universal criticality: random-bond model (B)

In order to simulate effects of random bonds in a sandpile automaton, we introduce a two-state variable $\boldsymbol{h} = (h_1, h_2)$ at each lattice site (i, j), where h_1 and h_2 are not necessarily integer. Each bond carries a quenched variable b with value $b = \pm 1$: the disorder here is that a random fraction c of the bonds have $b = -1$. The evolution rule for model B depends on the absolute value of the difference between components h_1 and h_2 at a site, which causes instability if it exceeds a critical value d_c. The entire number of particles then topple, and the two downstream neighboring sites are updated as follows (similar models were discussed earlier in Ref. [8]): If

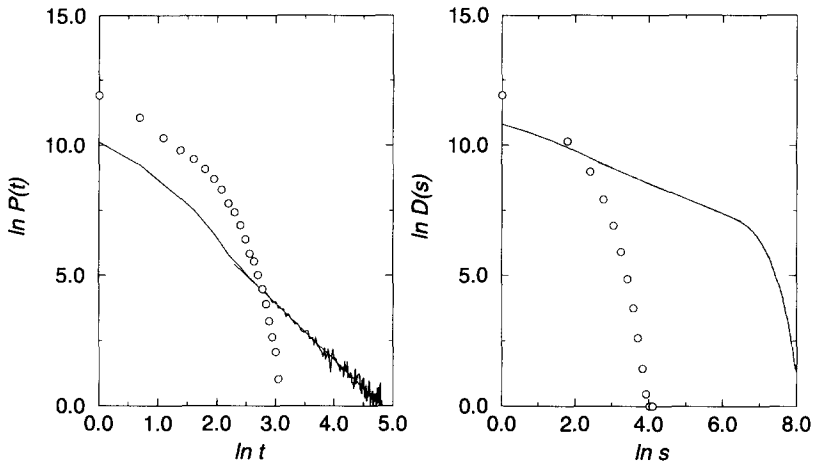

Fig. 3. Distributions of duration $P(t)$ and size $D(s \geq s_0)$ of the relaxation clusters in model B for conserving $\lambda = 1$ (solid lines) and nonconserving dynamics $\lambda < 1$ (open circles).

$$|h_1(i,j) - h_2(i,j)| \geq d_c, \tag{5}$$

then

$$h_1(i,j) \to 0, \qquad h_2(i,j) \to 0, \tag{6}$$

and

$$h_1(i+1, j\pm) \to h_1(i+1, j\pm) + (\lambda h_1(i,j) + h_2(i,j))/2, \qquad \text{if } b = +1, \tag{7}$$

$$h_2(i+1, j\pm) \to h_2(i+1, j\pm) + (\lambda h_2(i,j) + h_1(i,j))/2, \qquad \text{if } b = -1. \tag{8}$$

For $\lambda = 1$ the dynamics is conservative: all particles which leave site (i,j) appear at its neighbors. The instability condition Eq. (5) leads to a variety of states with high local values of h_1 and h_2. The asymptotic state is, however, SOC, and it appears that the precise form of the coupling between two states h_1 and h_2 is unimportant (see also Ref. [9]). Such a model incorporates some features of neural networks, and introduces frustration effects [8].

It is necessary to have conservative dynamics ($\lambda = 1$) in order for the system to self-organize into a critical state. Results of numerical simulations for the distributions of duration $P(t)$ and size $D(s \geq s_0)$ are shown in Fig. 3 for concentration $c = 0.5$, $\lambda = 1$ (solid lines) and $\lambda = 0.9$ (open circles). The present results average over simulations for a long time ($\approx 10^6$ steps) from several configurations, each of which is kept fixed for a particular simulation. The slopes of the straight lines in the case of conservative dynamics ($\lambda = 1$) determine the critical exponents according to $P(t) \sim t^{-(1+\theta)}$ and $D(s \geq s_0) \sim s^{-\tau}$. We find the best fit for $\theta = 1.040 \pm 0.018$ and $\tau = 0.650 \pm 0.028$. In this model the number of relaxed "particles" n is not proportional to the number of sites s at which relaxation occurs, thus leading to a new distribution $Q(n) \sim n^{-(1+\tau_n)}$. We also calculated $\langle n(l) \rangle$, to obtain the exponent μ defined in Eq. (3), as well as the average number of topplings in a cluster of a specified length l,

$$\langle n \rangle_l \sim l^{D_n}. \tag{9}$$

The scaling exponents are given in Table 1, and as we show in Section 5, they satisfy various scaling relations to within numerical error.

It appears that the exponents are independent of the concentration of defect bonds c, suggesting universal criticality. Similar robustness is exhibited by the system for variations in λ, provided that λ is strictly smaller than one: namely, all curves for $\lambda < 1$ coincide with the open circle curves in Fig. 3.

4. Nonuniversal criticality: random-slope model (C)

Model C combines the critical height model with a critical slope instability criterion at defect sites. At these sites, which are randomly distributed with relative concentration c, large columns of grains will form; these relax according to an alternative set of rules: if at least one of the two local slopes downstream of site (i, j) exceeds a critical value σ_c then toppling occurs towards these neighbors. If

$$\sigma_k(i,j) \equiv h(i,j) - h(i+1, j_k) \geq \sigma_c, \tag{10}$$

then

$$h(i,j) \to h(i,j) - 1, \qquad h(i+1, j_k) \to h(i+1, j_k) + 1, \tag{11}$$

where the index $k = \pm$ stands for right $(+)$ or left $(-)$ forward neighboring site. These rules are applied repeatedly until all slopes become subcritical. In order that topplings according to the critical height rule, where we set $h_c = 2$, do not affect those topplings that proceed through critical slope dynamics, we set $\sigma_c = 8 \gg h_c$. After some transient time local slopes $\sigma(i,j) \approx \sigma_c - 1$ are formed at randomly distributed defect sites, while the rest of the system topples according to the critical height rule. Due to the nonlocal character of the critical slope rule in Eqs. (10)–(11), topplings at defect sites may affect stability at their upstream neighbors too, and these sites might then topple in the next time step. In this way an internal time scale is introduced, although the macroscopic transport direction remains only one way, as in models A and B.

Results of the numerical simulations for the distributions of duration $P(t \geq t_0)$, size $D(s \geq s_0)$, and length $P(l)$ are shown in Fig. 4 for three concentrations of defect sites $c = 0.05$, 0.2, and 0.6. The exponents for this model, θ, τ, and α defined via $P(t \geq t_0) \sim t^{-\theta}$, $D(s \geq s_0) \sim s^{-\tau}$, and $P(l) \sim l^{-(1+\alpha)}$ respectively, have a (weak) concentration dependence. For instance, $\theta = 0.516 \pm 0.002$ for $c = 0.05$ increases to 0.581 ± 0.001 for $c = 0.6$. Similarly, $\alpha = 0.499 \pm 0.012$ at $c = 0.05$ changes to $\alpha = 0.563 \pm 0.024$ at $c = 0.6$, and $\tau = 0.354 \pm 0.001$ to $\tau = 0.427 \pm 0.001$ in the same region. For $c \geq 0.7$ the curves exhibit a finite curvature due to the multiple topplings. (The exponents given in Table 1 are for $c = 0.2$.)

The average duration of avalanches of selected length l, $\langle t \rangle_l$ in Fig. 4d, exhibits scale invariance, in agreement with the scaling properties of the distributions, namely

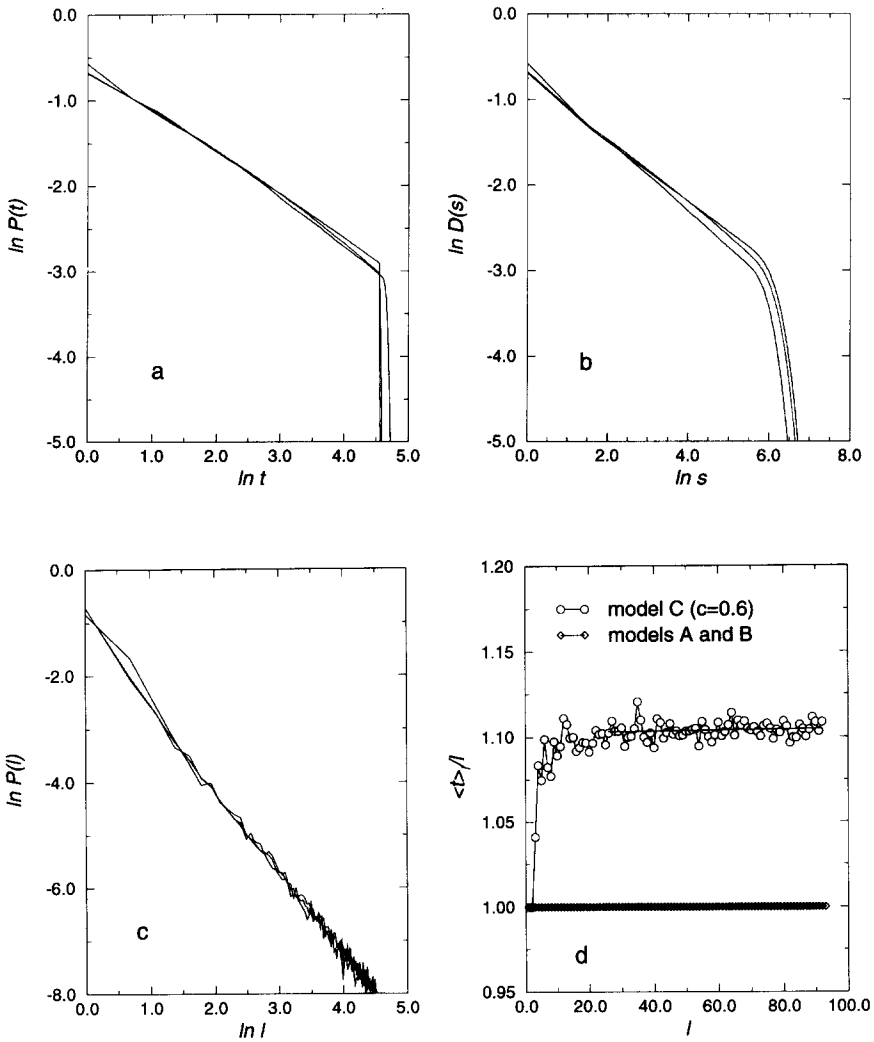

Fig. 4. Distributions of (a) duration, (b) size, and (c) length of the relaxation clusters for model C and (d) average duration of clusters of length l.

$$\langle t \rangle_l \sim l^z, \tag{12}$$

where z is the dynamic exponent. We find from Fig. 4d that $z = 1.013 \pm 0.001$ for $c = 0.6$. The dynamic exponent differs from 1 as a consequence of the nontrivial time scale in this model, although the values of the other exponents are close to (but, as our numerical results suggest, distinct from) the ones in the absence of defects. However, nonuniversal properties such as outflow current are different in the two cases: there are no apparent finite-size scaling effects in the presence of defects. In the limit $c \to 1$, all sites become subject to the critical slope rule, Eqs. (10)–(11), due to which a finite slope is formed. SOC is lost, since every avalanche is of infinite duration: the dynamics is dominated by single grain (one in/one out) events.

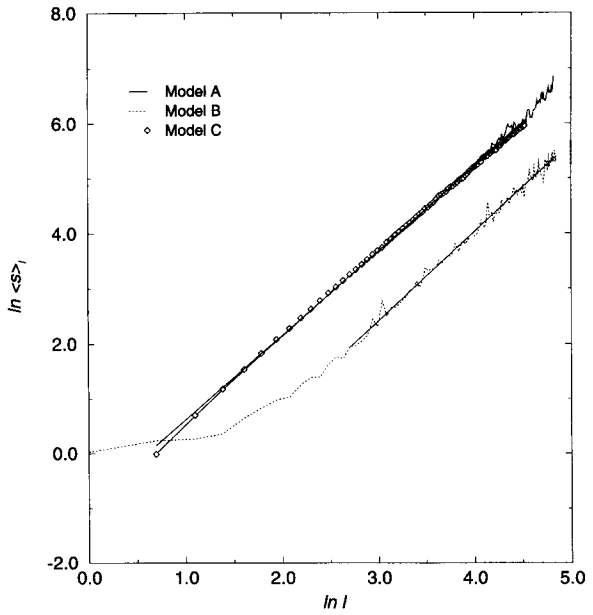

Fig. 5. Average size of the relaxation clusters $\langle s \rangle_l$ of selected length l, measured parallel to the transport direction, for models A, B, and C, as indicated.

5. Nonequilibrium phase transitions

In the preceding sections we have shown that sandpile automata are able to self-organize into a critical state in the presence of frozen-in random defects, provided that the dynamics conserves the number of grains at each time step. The sets of critical exponents for all three models are summarized in Table 1. For model A without defects the exponents are known exactly [2]. Model C exponents are for concentration $c = 0.2$ of defect sites. (Note that in models A and B time scale is measured in units of length, therefore the corresponding exponents are equivalent, i.e., $\alpha \equiv \theta$.) Also given is the mass-to-scale ratio $D_{||}$ defined with respect to the length parallel to the transport direction,

$$\langle s \rangle_l \sim l^{D_{||}}, \tag{13}$$

where $\langle s \rangle_l$ is the time-averaged size of clusters of selected length l. In Fig. 5, $\langle s \rangle_l$ is obtained from separate numerical simulations for models A, B, and C. The exponent D_n (cf. Eq. (9)) is also given in Table 1. The numerical values of the exponents are in reasonable agreement with the following scaling relation which can be shown to hold in all directed models:

$$\theta z = D_{||} \tau = D_n \tau_n = \alpha. \tag{14}$$

An order parameter which is appropriate for the defect-mediated phase transitions which occur in all three models can be defined as $q(c) = 1 - \langle J(c) \rangle / \langle J(0) \rangle$, with

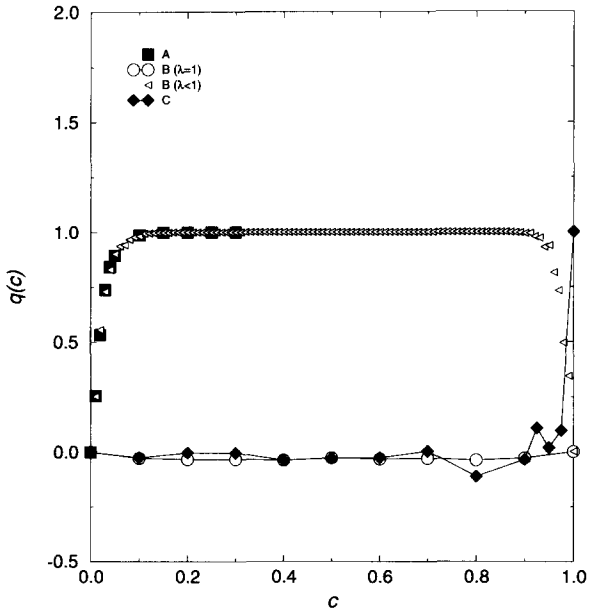

Fig. 6. Order parameter $q(c)$ vs. concentration of defects c for models A, B, and C, as indicated.

$\langle J(c)\rangle$ the outflow current, which is the total number of particles that flow over the lower boundary of the system in the presence of defects of concentration c. $\langle\cdot\rangle$ denotes an average over the total number of Monte Carlo steps.

In the models with conservative dynamics, i.e., model B with $\lambda = 1$ and model C, the average flux out of the system is balanced by the incoming current, thus leading to the vanishing of the order parameter in the self-organized critical state, as shown in Fig. 6. In model A, however, $\langle J(c)\rangle/\langle J(0)\rangle$ decreases due to nonconservation of number of particles at defect sites, leading to the appearance of finite order parameter q with increasing concentration of defect sites. For $c \geq c^* = 0.295 \equiv 1 - p_d$, the directed percolation threshold, the states are such that only finite avalanches occur, while for $c < c^*$ there are relaxation clusters of all sizes. The slope of the $q(c)$ curve at $c = c^*$ is close to zero. In this way, model A is subcritical for finite concentration c, which appears as a control parameter tuning the coherence length of the self-organized state. In the limit $c \to 0$ the coherence length diverges, as discussed in Section 2. Our numerical values indicate that the order-parameter curve approaches the vertical axis with a large but finite slope. We find the same phenomenon in model B with nonconserving dynamics ($\lambda < 1$), where transfer is incomplete at each negative bond. (Model B is symmetric with respect to transformation $c \to 1 - c$, reflecting the symmetry between positive and negative bonds, as can be seen in Fig. 6.)

There is another type of defect-mediated phase transition in model C in the limit $c \to 1$. At this point SOC is lost in favor of a state with finite net slope. This nonequilibrium phase transition requires a more detailed study. In the related case of annealed defects – when the probability of toppling p varies at each time step but is the same for all sites

in the system – a collective phase transition appears at $p_c = 0.293$ [10].

6. Summary

The presence of frozen-in defects in two-dimensional directed sandpile automata leads to various new phenomena. In this paper, we have introduced and studied three variations of the directed abelian sandpile automaton on the square lattice in order to explore this problem. We find that for site disorder, if the dynamics is nonconservative at defects, the system is driven into a subcritical state with a finite correlation length, which depends on the concentration c of defects. With any concentration of bond disorder, the correlation length remains finite and independent of the degree of nonconservation, provided that there is some loss of conservation, $\lambda < 1$. (Other models of nonconservative cellular automata have been studied recently [11], and are seen to have robust SOC behavior. Here we have lack of conservation occurring *solely* due to the presence of defects.) Furthermore, if the dynamics is conservative, the automaton self-organizes into a critical state with universal scaling properties. For a third type, the case of random slope defects, which correspond most closely to the random field version of analogous spin problems, we observe some indications of nonuniversal, concentration-dependent scaling exponents. Scaling relations between the exponents are fulfilled exactly for the first model (with $c = 0$), and within numerical error for the latter two models for each concentration of disorder. Finally, varying the concentration of defects appears to be a mechanism for continuously tuning the local rules of relaxation, which may eventually lead to a phase transition between metastable states with different properties.

Acknowledgements

This work was supported by the Ministry of Science and Technology of the Republic of Slovenia. We thank R. Pirc, J. Kertész and P. Grassberger for critical comments on the manuscript.

References

[1] P. Bak, C. Tang and K. Wiesenfeld, Phys. Rev. Lett. 59 (1987) 381;
P. Bak, C. Tang and K. Wiesenfeld, Phys. Rev. A 38 (1988) 364.
[2] D. Dhar and R. Ramaswamy, Phys. Rev. Lett. 63 (1989) 1659.
[3] S.S. Manna, L.B. Kiss and J. Kertész, J. Stat. Phys. 61 (1990) 923.
[4] B. Tadić, U. Nowak, K.D. Usadel, R. Ramaswamy and S. Padlewski, Phys. Rev. A 45 (1992) 8536.
[5] J. Theiler, Phys. Rev. E 47 (1993) 733.
[6] J.W. Essam, A.J. Guttmann and K. de'Bell, J. Phys. A 21 (1988) 3815.
[7] L.P. Kadanoff, S.R. Nagel, L. Wu and S.M. Zhou, Phys. Rev. A 39 (1989) 6524.
[8] E.N. Miranda and H.J. Herrmann, Physica A 175 (1991) 339;
B. Tadić, J. Non-Cryst. Solids 172–174 (1994) 501.

[9] G. Peng, Physica A 201 (1993) 573.
[10] S. Lübeck, B. Tadić and K.D. Usadel, in: Fractals in the Natural and Applied Sciences, ed. M.M. Novak (Chapman & Hall, London, 1995), and to be published.
[11] See e.g., K. Christensen and Z. Olami, Phys. Rev. A 46 (1992) 1829;
A. Corral, C.J. Pérez, A. Díaz-Guilera and A. Arenas, Phys. Rev. Lett. 74 (1995) 118.